Comparison between Soft and Hard Decision Decoding using Quaternary Convolutional Encoders and the Decomposed CPM Model

Manjeet Singh (ms308@eng.cam.ac.uk)
Ian J. Wassell (ijw24@eng.cam.ac.uk)
Laboratory for Communications Engineering
Department of Engineering
University of Cambridge

ABSTRACT

A generic M-ary continuous phase modulation (CPM) scheme, with a modulation index of h = 1/M, can be decomposed into a continuous-phase encoder (CPE) followed by a memoryless modulator (MM), where the CPE is linear over the ring of integers modulo M. By using a channel encoder (CE), which is a convolutional encoder, to operate over the same ring of integers modulo M, the CE and the CPE can be combined to create another convolutional encoder called an extended CE, so called, as the CPE is now an extension of the CE. In this paper, a ½ rate CE over the ring of integers modulo 4 is combined with the CPE of a quaternary CPM scheme whose modulation index h = ¼. Using this trellis coded modulation design, the paper compares the performance of soft and hard decision decoding of a serially concatenated channel coded system, where the inner encoder is the quaternary extended CE and the outer encoder is another quaternary convolutional encoder. Although simulations show the superiority of soft decision decoding, good results were obtainable from hard decision decoding.

I. INTRODUCTION

Since the pioneering work of Ungerboeck in 1982, trellis-coded modulation (TCM) has become an effective coding technique for bandlimited channels. By using TCM with memoryless modulations, such as *M*-ary phase shift keying (MPSK) or quadrature amplitude modulation (QAM), significant coding gains can be achieved without bandwidth expansion. Studies have also been done that combine encoders with memory modulation schemes [1]. One such scheme is continuous phase modulation (CPM).

The useful of CPM in digital mobile systems stems from the fact that it provides a good trade-off between power and spectrum efficiency, for a given bit error rate. Its constant envelope permits the use of non-linear Class C amplifiers, which are 2dB to 3dB more power efficient than Class A or AB power amplifiers demanded by modulation schemes with non-constant carrier amplitudes. In addition, the "smoothness" of the carrier phase change permits a higher spectral efficiency to be achieved compared with conventional phase shift keying (PSK), where "abrupt" phase changes occur. Hence, CPM is particularly suited for mobile wireless transmission, where power and spectrum efficiency are required.

On the other hand, compared with QPSK for example, the initial definition of CPM does not naturally lend itself to be combined with coding because it cannot directly accept symbols belonging to the ring of integers Z_m, where M is the ring size, e.g. $Z_4 = \{0, 1, 2, 3\}$. To over come this, Rimoldi [2] proposed a decomposed CPM model which allowed a "natural" attachment to a convolutional encoder operating over the same ring of integers. Also, unlike earlier CPM representation [3, 4], the decomposed model produced a time invariant phase trellis, thus reducing the complexity in both the transmitter and receiver.

II. DECOMPOSED CPM MODEL

It has long been known that bandwidth of CPM schemes could be reduced by smoothing the variations of the information-carrying phase. This can be done by shaping the phase using an analog filter. The model generally used is shown in Figure 1.

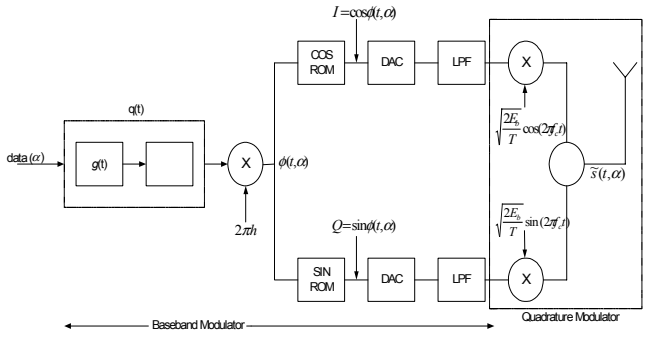

Figure 1. CPM modulator schematic

Besides providing spectral economy, CPM systems have an inherent "coding structure" when compared to PSK modulations. This "coding structure" is due to the memory that is introduced by the phase-shaping filter and the decoder can exploit this. Rimoldi believed that the model generally used for CPM (shown in Figure 1) was unsatisfactory as an *analog* phase-shaping filter describes the key aspect of the *digital* modulator i.e. the memory it introduces.

Massey [5] suggested that a CPM scheme could be decomposed into two parts: a continuous phase encoder (CPE) with memory, and a memoryless modulator (MM). Such decomposition has two advantages [2]. Firstly, the "encoding" operation can be studied independently of the modulation. The second advantage is that the isolation of the MM would allow the cascade of the MM, the waveform channel (e.g. additive white Gaussian noise (AWGN)) and the demodulator to be modeled as a discrete memoryless channel.

In [2, 6, 7], Rimoldi derived a generic decomposition model of an *M*-level CPFSK, comprising a CPE and an MM as shown in Figure 2. He showed that the CPE is a linear (modulo some integer *M*) time-invariant encoder and the MM another time-invariant device. It is then of interest to optimally combine a convolutional coder with the CPE to create a trellis coded modulation scheme.

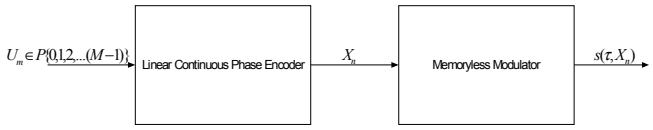

Figure 2. Block diagram of CPM system decomposed into a linear continuous phase encoder and a memoryless modulator

[8] provides a list of convolutional channel encoders (CE) that are suitable for combination with the CPE without the use of a mapper. To facilitate this, the CE must operate over the same algebra structure as the CPE. This is unlike the usual approach where mappers are pertinent [1, 9].

In this research, we combine a quaternary CE and CPE, both operating over the ring of integers modulo 4. This combination is called an extended CE and is effectively a quaternary convolutional encoder. We compare the performance of 2 decoding techniques-hard and soft decision decoding using a serially concatenated channel-coding (SCCC) scheme. The outer encoder is a ½ rate quaternary convolutional encoder also operating over the ring of integers modulo 4, while the inner encoder is a ½ rate quaternary extended CE. The CPM uses has a raised cosine (2*RC)* filter and has a modulation index of $h = ¼$.

Both the decoding techniques are based on the Viterbi algorithm. For the soft decision decoding (SDD) technique, the soft output information from the inner Soft-Output Viterbi Algorithm (SOVA) was used to enhance the performance of the outer soft input Viterbi decoder. Block and convolutional interleavers of various sizes, to permutate the outer codeword symbols, were investigated.

III. SYSTEM DESIGN

The section explains the design of the outer encoder, extended CE, the memoryless modulator and the decoders. Figure 3 shows the set-up of the SCCC scheme.

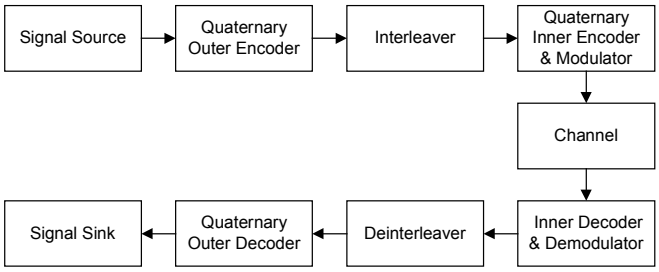

Figure 3. Generic block diagram of the serially concatenated channel-coding scheme.

For both decoding techniques the outer encoder is a quaternary convolutional encoder while the inner encoder is the extended CE. The modulator is the memoryless modulator.

In the case of hard decision decoding (HDD), the inner decoder/demodulator only output hard decision code symbols to be decoded by the quaternary outer decoder. For SDD, apart from outputting hard decision symbols, the inner SOVA decoder also provided reliability information that was used by the soft input outer decoder to enhance its decoding performance

A. Design of the extended CE

Figure 4 shows the design of the extended CE. For the purpose of system evaluation, a 2*RC* (partial-response) scheme with $h = ¼$ ($M = 4$) was implemented using the baseband decomposed CPM model. The CPE has two memory (delay) cells. One cell stores the previous transmitted symbol while the other memory cell stores the sum (mod 4) of all previously transmitted symbols. As the phase response of the incoming signal lasts two symbol intervals ($L = 2$), "controlled" intersymbol interference is introduced.

The extended CE is a ½ rate quaternary convolutional encoder. It has 3 memory cells (memory cells D1 and D2 form part of the CPE) and generates 64 states (4^3). As there are 4 branches/ waveforms emanating from and arriving at each state and each "analog" waveform is made of 8 samples, a total of 8 X 4 X 64 = 2048 waveform samples would require processing for the extended CE at each iteration of the Viterbi algorithm.

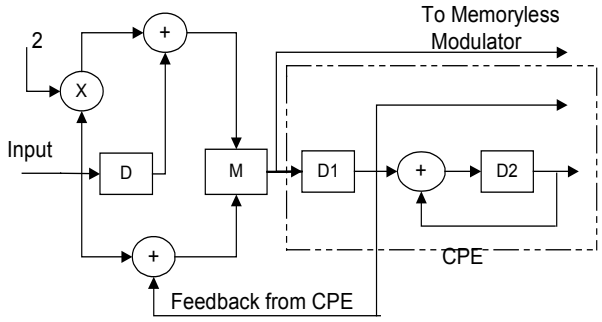

Figure 4. ½ rate extended CE with feedback from the CPE. D denotes a memory cell while M denotes a multiplexer. Additions are all modulo 4. D1 and D2 are the memory cells of the CPE.

As both the CE and CPE operate over the same algebra, no mapper is required to link them. This allows the state of the CPE to be fed back and be used by the CE enabling the use of a CE with a shorter constraint length. Such a combination is called an extended CE, as the CPE is now an extension of the CE.

B. Design of the Memoryless Modulator

The raised cosine (*RC*) phase shaping function is implemented using two finite impulse response (FIR) digital filters, FIR filter A and FIR filter B as shown in Figure 5. In this study, each output waveform is made up of eight samples.

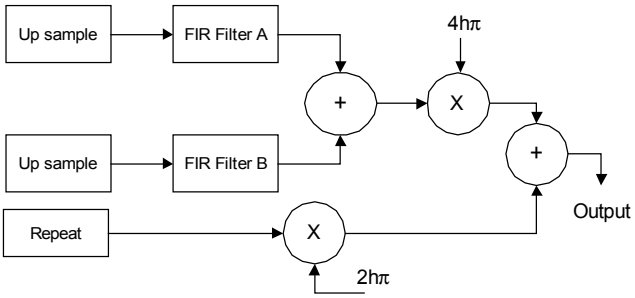

Figure 5. Block diagram of the memoryless modulator. The Up Sample and Repeat blocks increase the samples of the input signals by a factor of 8. h denotes the modulation index.

C. Design of the Outer Encoders

The design of the quaternary outer convolutional encoder is shown in Figure 6 below. Its design is similar to the extended CE shown in Figure 4 except for outputs to the memoryless modulator.

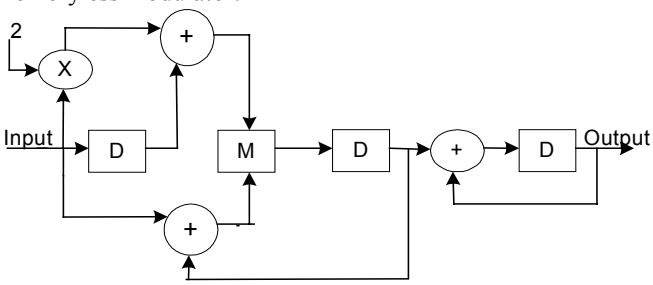

Figure 6. ½ rate quaternary outer encoder. D denotes a memory cell while M denotes a multiplexer. Additions and multiplications are modulo 4.

D. Design of the Viterbi Decoders

A general overview of the Viterbi decoder is shown in Figure 7. The design of both the hard decoder and the SOVA is basically the same.

The decoding is based on a technique called *list decoding*, whereby a list of all the waveforms the transmitter can generate are stored in a ROM in the decoder.

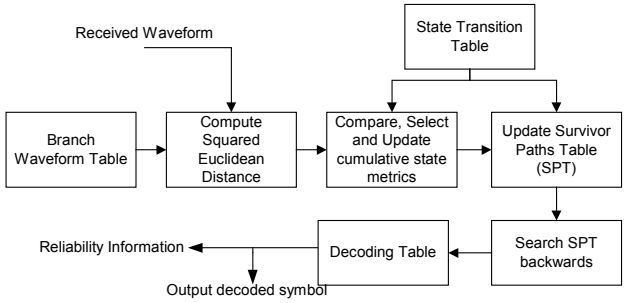

Figure 7. High-level diagram of the Viterbi Decoders

When a waveform is received, (corrupted by additive noise or fading), the Euclidean distances (ED) between it and the waveforms in the list are calculated. The waveform having the smallest ED from the received waveform is chosen from the list and processed. These distances (or branch metrics) serve as a probability that a given waveform/symbol was actually sent. However, these branch metrics are not used in isolation. They are used in conjunction with the probabilities (state metrics) associated with the states of the trellis that each of the branches depart from. In this way, the Euclidean

distance between the entire received sequence and the most likely path through the trellis can be calculated on a symbol-by-symbol basis.

To facilitate computation of the most likely path through the trellis, both the inner and outer decoders contain three tables. For the outer decoding, the tables are generated only by the outer encoder. For the inner decoding, the tables are generated by the extended CE and the MM. The three tables are:

a. State Transition Table - which takes as its inputs the current state and input symbol and outputs the next state.

b. Waveform Table – which takes as inputs the current state and symbol input and generates the output waveform. This table contains the list of all the waveforms that can be generated by the encoder.

c. Decoding Table – which takes as its inputs the current state and previous state and outputs the transmitted symbol.

It is assumed that there are no parallel transitions between states. The advantage of using these tables is that for the same value of L the Viterbi decoders need not be redesigned for each new scheme to accommodate more or less states or a different symbol alphabet size.

Apart from outputting the decoded symbol, the SOVA, in the first configuration, also outputs reliability information, which is used to improve the performance of the outer decoder. As there are 4 branches departing and arriving at each state, the reliability information was calculated based on the lowest and highest cumulative metric through the trellis. This reduced the complexity of the decoders considerably.

IV. SIMULATIONS AND RESULTS

The entire coding system was built in software and tested using Monte Carlo based simulations. The results obtained are in terms of the bit error rate (BER) as a function of the signal to noise ratio (SNR).

In all the simulations, a normalized bandwidth of $BT_s = 1.2$ was assumed where B is the bandwidth and T_s the symbol duration. For the quaternary $2RC$ scheme, this bandwidth contains approximately 99.97% of the total power. The overall code rate of the SCCC scheme is ¼ (both the inner and outer encoders have a code rate of ½). Both the inner and outer encoders have 64 states.

Results of the HDD and SDD simulations in an AWGN channel using a 10 x 10 block interleaver are shown graphically in Figures 8.

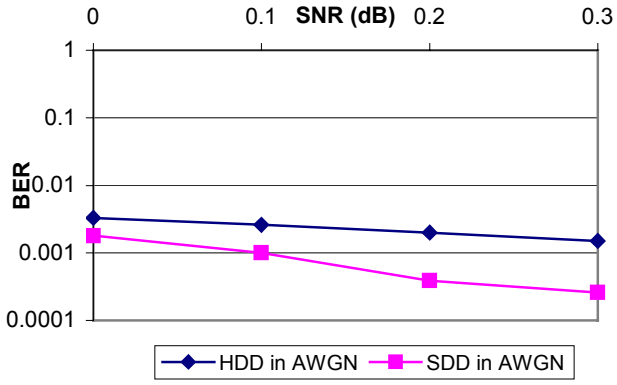

Figure 8. Performance of HDD and SDD in an AWGN channel.

Summarized in Tables 1 and 2 are some pertinent BER results regarding SDD and HDD respectively. All simulations are executed over an AWGN channel. Simulations using convolutional interleavers gave approximately the same results as those for block interleavers.

SNR	Interleaver Size	BER
1.6dB	no interleaver	1.4×10^{-4}
0.3dB	10 x 10 block interleaver	2.6×10^{-4}
0.0dB	10 x 10 convolutional interleaver	7.9×10^{-4}
0.3dB	10 x 10 convolutional interleaver	3.5×10^{-4}

Table 1. Soft decision decoding results

SNR	Interleaver Size	BER
1.6dB	no interleaver	1.4×10^{-4}
0.5dB	10 x 10 block interleaver	5.0×10^{-4}
0.2dB	50 x 50 block interleaver	9.9×10^{-5}
0.5dB	10 x 10 convolutional interleaver	5.7×10^{-4}

Table 2. Hard decision decoding results

The results clearly show the superiority of SDD over HDD. However, the latter did produce some very good results e.g. with a 50 x 50 block interleaver, a BER of approximately 9.9×10^{-5} was achievable.

V. DISCUSSION AND CONCLUSION

Previous works [2, 6] have suggested decomposing a CPM modulator and combining the CPE with a CE naturally i.e. without a mapper. To enable this, both the CE and the CPE must operate over the same algebra structure. In our

research, we have designed an SCCC scheme using the decomposed CPM model and convolutional encoders and tested it in AWGN conditions.

The results show the superiority of SDD over HDD. These good results were achieved without the use of iterative decoding, which can introduce high latency, depending on the number of iterations, during decoding. The main potential areas of application of these configurations are the improvement of already established standards, for example GSM and cellular digital packet data.

VI. ACKNOWLEDGEMENTS

The authors would like to thank the Laboratory for Communications Engineering (Cambridge University) for the use of their equipment in the research and the Center for Wireless Communications (National University of Singapore) for their assistance.

VII REFERENCES

[1] J.B. Anderson, T. Aulin and C.E. Sundberg, "*Digital Phase Modulation*", New York: Plenum, 1986.

[2] B. Rimoldi, "*A decomposed approach to CPM*," IEEE Trans. Inform. Theory, vol.34, pp.260-270, Mar.1988.

[3] T. Aulin and C. –E. W. Sundberg, "*Continuous Phase Modulation – Part I: Full response signaling*", IEEE Trans. Commun., vol. COM-29, pp. 196-209, Mar.1981.

[4] T. Aulin, N. Rydbeck and C. –E. W. Sundberg, "*Continuous Phase Modulation – Part II: Partial response signaling*", IEEE Trans. Commun., vol. COM-29, pp. 210-225, Mar. 1981.

[5] J.L Massey, "*The how and why of channel coding*," in Proc. Int. Zurich Seminar, Mar.1984, pp. F11(67)-F17(73).

[6] B. Rimoldi, "*Continuous phase modulation and coding from bandwidth and energy efficiency*," PhD dissertation, Swiss Fed. Inst. Technol., 1988.

[7] B. Rimoldi, "*Design of coded CPFSK modulation system for bandwidth and energy efficiency*," IEEE Trans.Commun., vol.37, pp. 897-905, Sept.1989.

[8] Quinn Li, "*On bandwidth and energy efficient digital modulation schemes*," PhD dissertation, Sever Institute, University of Washington, 1996.

[9] S.V. Pizzi and S.G. Wilson, "*Convolutional coding combined with Continuous Phase Modulation*," IEEE Trans. Commun., vol.33, pp.20-29, Jan.1985.